Biocompatible and degradable gelatin dielectric based low-operating voltage organic transistors for ultra-high sensitivity NH_3 detection

Xinming Zhuang, Dayong Zhang, Xiaolin Wang, Xinge Yu, and Junsheng Yu

Citation: Appl. Phys. Lett. **113**, 263301 (2018); doi: 10.1063/1.5054026
View online: https://doi.org/10.1063/1.5054026
View Table of Contents: http://aip.scitation.org/toc/apl/113/26
Published by the American Institute of Physics

Biocompatible and degradable gelatin dielectric based low-operating voltage organic transistors for ultra-high sensitivity NH_3 detection

Xinming Zhuang,[1] Dayong Zhang,[1] Xiaolin Wang,[1] Xinge Yu,[2,a)] and Junsheng Yu[1,a)]
[1]*State Key Laboratory of Electronic Thin Films and Integrated Devices, School of Optoelectronic Science and Engineering, University of Electronic Science and Technology of China (UESTC), Chengdu 610054, Peoples Republic of China*
[2]*Department of Biomedical Engineering, City University of Hong Kong, Hong Kong, Peoples Republic of China*

(Received 28 August 2018; accepted 28 November 2018; published online 26 December 2018)

We developed an ultra-high sensitive ammonia (NH_3) gas sensor that incorporates a biocompatible/degradable gelatin dielectric layer in a top-contact organic thin-film transistor. The sensitivity study of the gas sensor involves detecting the saturation current change with analyte concentrations, exhibiting a saturation current changing from 17.6% to 45.1% for the concentration of NH_3 from 500 ppb to 30 ppm. Importantly, this type of sensing platform shows an excellent detecting limit of 174.0 ppb with a low operating voltage of 4 V. To understand the mechanism of this phenomenon, we fabricated another group of devices that incorporates an additional thin layer of polystyrene covered on top of the gelatin layer. The response sensitivity of this type of sensor is only 5.1% for the NH_3concentration of 30 ppm. Systematic studies including morphology analysis of the organic films and electrical properties of the sensors were performed. The results indicate that the functional groups on the gelatin dielectric surface groups have ability to adsorb NH_3 analyte, thereby leading to a superior sensing performance. This work demonstrates that the biocompatible/degradable gelatin with unique functional groups is applicable for readily manufacturable low-operating voltage and high-performance thin-film transistor-based gas sensors. *Published by AIP Publishing.* https://doi.org/10.1063/1.5054026

With the advent of the Internet of Things (IoT) era, more and more emphasis is placed on the humanization and portability of electronic products. Meanwhile, in order to protect the nature environment and human race, developing low-cost, efficient, and low-loss gas sensing devices for monitoring pollutant gases, especially the harmful and toxic gases, becomes an urgent topic.[1–3] Among various gas sensing devices, organic thin-film transistor (OTFT)-based sensors have attracted intriguing attention due to their advantages of lightweight, flexibility, and low material/process costs.[4–6] Moreover, by virtue of the field effect tuned multiple electrical parameters, OTFTs can function as both signal transducers and amplifiers. Therefore, OTFTs are widely adopted as the unit component of high performance sensors.[7–11]

Toxic gas ammonia is one of the major industrial chemical products, which is detrimental to human health and environmental issues. Long-time ambient NH_3 exposure, even very low NH_3 concentration (ppb level), can cause asthma, severe respiratory inflammations, and lung diseases.[12,13] Therefore, developing low cost and high sensitivity NH_3 gas sensors becomes a significant topic, and a lot of research efforts has been devoted to enhancing the NH_3 sensing property of OTFT-based sensors.[14–16] For example, Khim *et al.* demonstrated flexible, highly sensitive NH_3 gas sensors with ultrathin donor-acceptor (D-A)-type semiconducting conjugated polymers.[17] Introducing a tris(pentafluorophenyl)borane (TPFB) compound in a semiconducting layer as the receptor of NH_3 is another route for detecting low concentration NH_3.[18] Besides the development of semiconducting materials, high-performance OTFT-based gas sensors can also be realized by introducing an additional function layer.[19] However, most reported OTFT-based NH_3 sensors mainly focus on developing semiconductor engineering but neglects the problem of high driven voltages.[20,21] Developing and engineering dielectric layers in OTFT-based sensors is the most straightforward route to lower power consumption. Due to the fact that charge carrier transportation in OTFT mainly occurs at the interface between a semiconductor and a dielectric layer, a proper dielectric layer may also determine the sensing property.[5,22]

On the other hand, with the rapid development of biodegradable and wearable electronics, bio-compatible materials show immense potential in next-generation electronics.[23,24] Some naturally existing biological materials, such as silk fibroin, chicken albumen, DNA, and RNA, have attracted intriguing attention owing to their advantages of biodegradability, biocompatibility, environmental friendliness, and abundance.[25,26] Among them, Gelatin, obtained from bones and skins of the animals, a kind of natural protein, has been widely used for biological detections in recent years.[27–29] A large number of studies verified that gelatin not only contains plenty of chemical groups but also exhibits excellent dielectric properties.[30] The application of gelatin as the dielectric layer in high performance OTFTs was also reported.[31] Consequently, gelatin shows enormous potential of

a)Authors to whom correspondence should be addressed: xingeyu@cityu.edu.hk, Tel.: 852-3442-9525 and jsyu@uestc.edu.cn, Tel.: 86-28-83207157.

application in biocompatible/biodegradable OTFT-based sensors. Nevertheless, reports on gelatin-based gas sensors are rarely seen.

In this work, we present a simple OTFT-based NH_3 sensor platform with biocompatible/degradable gelatin as dielectric layers, which provides a low-power consumption route for ultra-sensitive detection of NH_3 gas. As a comparison, OTFT gas sensors with conventional polyester dielectrics were also studied, and these devices show much poorer performance in NH_3 sensing than those gelatin-based ones. The functional groups on the gelatin dielectric surface exhibit the ability of NH_3 absorption, thus resulting in superior NH_3 gas responsivity and selectivity of the gelatin-based devices. With the contribution of the high capacitance of the gelatin dielectric layer, the operating voltage of the OTFT-based NH_3 sensor is as low as -4 V. The results establish considerations in design for low-cost, biocompatible/degradable sensors.

Figure 1(a) shows the schematic diagram of a top-contact (TC) OTFT-based NH_3 sensor with biocompatible/degradable gelatin as the dielectric layer. Indium tin oxide (ITO)-coated glass used as the substrate and the gate electrode was cleaned in an ultrasonic bath with detergent, acetone, deionized water, and isopropanol for 15 min each. Gelatin (extracted from animal skin, Sigma-Aldrich) was dissolved in deionized water with a concentration of 50 mg/ml. Next, a 400 nm thick gelatin dielectric layer with a unit capacitance of 18.7 nF/cm^2 (shown in Fig. S1, supplementary material) was spun-coated at 2000 rpm for 1 min and then baked on a hot plate at 80 °C for 15 min to remove the residual solvent. Then, a 30 nm thick pentacene semiconducting layer (purchased from Tokyo Chemical Industry Co., Ltd) was vacuum deposited on the gelatin dielectric layer under 2×10^{-4} Pa at a rate of 0.2 Å/s. Finally, 30 nm thick Au source and drain electrodes were thermally evaporated using a shadow mask at a rate of 0.2 Å/s under 3×10^{-3} Pa. The channel width/length ratio was 100 ($W = 10$ mm, $L = 100$ μm). The OTFT-based sensor was put in an airtight test chamber (approximately 2 ml) for sensing property testing. Dry air and 100 ppm standard NH_3 gas (anhydrous, Sichuan Tianyi Science & Technology Co.) were mixed to form various concentrations ranging from 0 to 30 ppm and then introduced into the test chamber by a mass flow controller. Capacitance measurements of the gate gelatin and gelatin/PS dielectrics were performed by sweeping the capacitance-frequency properties from a metal-insulator-semiconductor (MIS) architecture, specifically, ITO/Gelatin/Au and ITO/Gelatin/PS/Au, using an Agilent 4294A (Santa Clara, CA, USA). The gas sensing characteristic of these devices was measured using a Keithley 4200 sourcemeter at room temperature.

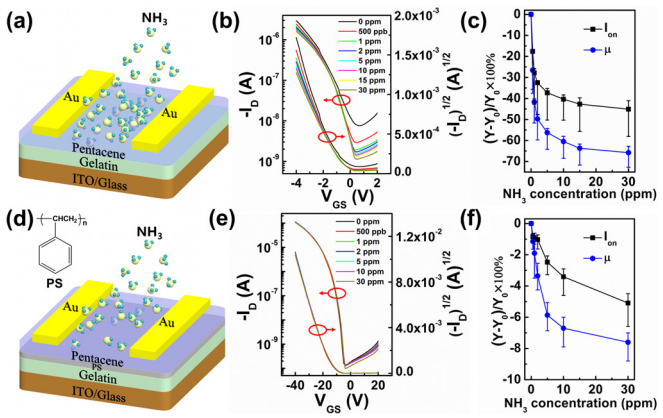

FIG. 1. (a) Schematic illustration of a NH_3 sensor in an OTFT architecture with gelatin as the dielectric layer. (b) Typical transfer curves of the gelatin-based OTFT at specific concentrations of NH_3 ($V_{DS} = -4$ V). (c) Variation of saturation current I_{on} and mobility μ of the gelatin-based OTFT at different NH_3 concentrations. (d) Schematic illustration of the NH_3 sensor with gelatin/PS as the dielectric layer. (e) Typical transfer curves of the gelatin/PS-based OTFT at specific concentrations of NH_3 ($V_{DS} = -40$ V). (f) Variation of I_{on} and μ of gelatin/PS-based OTFT at various NH_3 concentrations.

The transfer curves with a source-drain voltage (V_{DS}) of -4 V were used for characterizing the sensing properties of the OTFT-based sensor. Figure 1(b) shows a set of transfer curves correlated with the sensor at various concentrations of NH_3 exposure. For the *I-V* response to different concentrations of NH_3, the device was exposed to each tested concentration of NH_3 for 2 min before measurement. The transfer characteristics clearly demonstrate that gelatin-based OTFT exhibits an excellent NH_3 response sensitivity. As another important index of sensing sensitivity, the field-effect mobility (μ) of the OTFTs will be discussed next. μ can be extracted in the saturation regime by using the following equation:

$$I_D = (W/2L)\mu C(V_{GS} - V_T)^2, \tag{1}$$

where L and W are the channel length and width, respectively. C is the capacitance (per unit area) of the dielectric layer, and V_{GS} is the gate voltage. To intuitively discern sensing properties, the variation of I_{on} and μ, defined as $Y = |(Y_{NH3}\text{-}Y_0)/Y_0| \times 100\%$, is presented in Fig. 1(c). In this work, over 100 devices were fabricated, and their transistor performance is very consistent. Due to the long duration data collection time, here we summarized an average value of five representative samples. Y of I_{on} of the gelatin-based sensors exhibits a changing range of 41.9% to 58.2% for 30 ppm NH_3. A similar trend of μ in these devices was also observed, with a changing range of 62.2% to 73.1% for 30 ppm NH_3. The means of decrease in I_{on} and μ of the gelatin-based OTFTs are 45.1% and 65.8% when exposed to 30 ppm NH_3, respectively. Notably, the I_{on} and μ values of these devices still show a decrease of 17.6% and 26.6% when exposed to 500 ppb NH_3. Meanwhile, the response time and recovery time were also tested by real-time sensitivity testing, as shown in Fig. S2, supplementary material. The response time and the recovery time are 15.4 s and 42.2 s, respectively. Further tests were also performed on lower NH_3concentrations for the purpose of estimating the limit of detection (LOD) using the linear fitting method shown in the following equation:[5]

$$Y_{LOD} = \frac{-a \times b + \sqrt{a^2 \times b^2 - (b^2 - \eta^2 \times \Delta b^2)(a^2 - \eta^2 \times \Delta a^2)}}{b^2 - \eta^2 \times \Delta b^2}, \tag{2}$$

where $\eta = 1.96$ corresponds to the 95% confidence level; a, b, Δa, and Δb are the parameters extracted from the linear fit

of Fig. S3, supplementary material. The estimated LOD of the sensor in this work is 174.0 ppb, indicating that the sensor can effectively monitor trace amounts of NH_3 in the practical environment.

To understand the reason for superior gas-sensing properties, comparable and parallel studies were carried out by investigating the influence of different dielectrics on the performance of OTFT-based sensors. Here, we fabricated another group of OTFT devices with the same structure but covering the gelatin layer by a thin film of polystyrene (PS), as shown in Fig. 1(d). The fabrication process started with dissolving PS (average Mw ∼ 290k, Sigma-Aldrich) in xylene (Tokyo Chemical Industry Co., Ltd.) with a concentration of 3 wt. %, spin-coated onto the gelatin layer at 5000 rpm for 1 min, and baked in an oven at 130 °C for 1 h. After covering the thin PS (100 nm thick) layer, the OTFT cannot embody a transistor feature under operating voltage of −4 V (V_{GS} and V_{DS}) due to the decrease in the capacitance of the dielectric layer. Instead, the operating voltage was increased up to −40 V. These OTFTs with the gelatin/PS dielectric layer were tested at various NH_3 concentrations. As shown in Figs. 1(e) and 1(f), the variations of I_{on} and μ of the gelatin/PS devices are only 5.1% and 7.6% when exposed to 30 ppm NH_3, respectively, while the I_{on} and μ values just exhibit slight changes of 0.8% and 1.1% for 500 ppb NH_3, respectively.

The sub-threshold slope (*SS*) is another significant parameter to characterize the sensing properties in OTFT-based sensors since the *SS* reflects the charge trap density (N) at the interface between the dielectric and organic semiconductors. N can be extracted using the following equation:[8]

$$SS = (kT/q)\ln 10(1 + qN/C), \tag{3}$$

where q is the electronic charge, k is Boltzmann's constant, T is the absolute temperature, and C is the areal capacitance of the dielectric. The *SS* of gelatin/PS-based OTFT shows a negligible change at different NH_3 concentrations, which means that the NH_3 analyte does not change the trap state at the interface between PS and pentacene. In contrast, the *SS* of gelatin-based OTFT has remarkable response with the introduction of NH_3 analyte. Such a result implies that plenty of NH_3 molecule is adsorbed at the interface and interacts with trapping charge carriers. Based on the above results, it can be seen that sensing performance of gelatin-based OTFT is much greater than that of the gelatin/PS-based OTFTs. Compared to gelatin/PS-based OTFT, a 21× greater response sensitivity in gelatin-based OTFT was observed. It is noteworthy that the operating voltage of the device with the gelatin dielectric layer is only −4 V.

To disclose the origin of sensing performance enhancement, the surface topographies of the gelatin film, the gelatin/PS film, and pentacene films (on top of the dielectrics) were first probed by atomic force microscopy (AFM) (Agilent, AFM 5500). It is well known that the morphologies of both dielectric and organic films could significantly affect the sensitivity.[8,22] As shown in Figs. 2(a) and 2(b), the gelatin film and the gelatin/PS film show similar morphologies, with the root mean square roughness (RMS) of 0.49 nm and 0.45 nm, respectively. Pentacene films deposited on top of

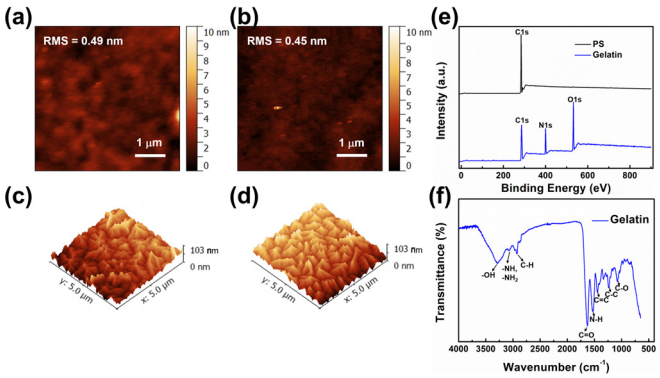

FIG. 2. (a) AFM images of the films of (a) gelatin, (b) gelatin/PS, (c) pentacene deposited on gelatin, and (c) pentacene deposited on gelatin/PS. (e) XPS of gelatin and PS films. (f) FTIR spectroscopy of gelatin.

dielectrics exhibit similar crystal growth as shown in Figs. 2(c) and 2(d). The grain size of pentacene deposited on the gelatin film is slightly larger than that on the gelatin/PS film. The results of the topographies indicate that film roughness and gaps in-between pentacene grains are not the dominating factors for sensitivity improvement.[32,33] The analyte-caused capacitance change of the dielectric layer in OTFT-based sensors is also a well-known mechanism. Here, the capacitances of the gelatin are tested by the static testing method before and after NH_3 (1 ppm) introduction to verify if any swelling occurred on gelatin, as shown in Fig. S4, supplementary material. The results show that the capacitances are almost unchanged.

Therefore, the surface properties of the gelatin are confirmed to be the main contribution to the sensitivity enhancement. X-ray photoelectron spectroscopy (XPS) (Omicron ESCA Probe, Tokyo, Japan), a powerful surface characterization tool, was next utilized to analyze the surface chemical elements of the dielectrics. Three dominant peaks at ∼286, ∼400, and ∼532 eV in the XPS survey spectrum depicted in Fig. 2(e) were related to C 1s, N 1s, and O 1s species, respectively. This result implies that the gelatin contains a lot of functional organic chemical groups. The gelatin film was next analyzed by Fourier transform infrared (FTIR) spectroscopy (Thermo Scientific, Nicole-10) to further identify these functional organic chemical groups. As shown in Fig. 2(f), clear vibrational peaks at ∼1078, ∼1334, ∼1535, ∼2927, and ∼3285 cm^{-1} can be observed, which correspond to C-O, C = C, C = O, -NH, and -OH, respectively.[29,34] The combination of these polarization chemical bonds forms functional groups, which could interact with NH_3 analyte. When the polar molecules NH_3 diffuse into the interface of gelatin/pentacene, the functional group on the gelatin would trap more NH_3 molecules, thus restraining charge carrier transport in the conducting channel. As a result, a large amount of free hole carriers will be fettered by electron donors.[35,36] As shown in Figs. 3(a) and 3(b), compared to the PS film, the gelatin film will absorb more NH_3 due to the existence of functional groups. In contrast, such interaction will not occur between NH_3 and benzene rings.[20] Therefore, the trapped NH_3 at the interface of gelatin/pentacene effectively reduces the magnitude of the source-drain current and charge carrier mobility.

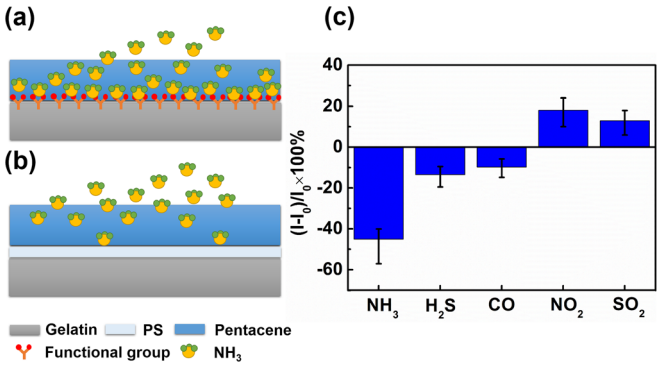

FIG. 3. (a) and (b) Schematic illustration of the NH_3 diffusion and absorption processes resulting from functional groups in different devices. (c) Percentage I_{on} variation of OTFT with the gelatin dielectric layer upon exposure to 30 ppm different gas analytes.

Considering practical applications, selectivity of gas sensors is an open matter for evaluating the possibility of commercialization.[37,38] So, we investigate the response of gelatin-based OTFT to several representative coexisting air pollutions including NH_3, H_2S, CO, NO_2, and SO_2. As shown in Fig. 3(c), it is clear that the response of NH_3 is at least 2.5× times greater than all the other gases: the responsivities to H_2S, CO, NO_2, and SO_2 under 30 ppm are 13.5%, 9.8%, 18.0%, and 12.9%, respectively. It is apparent that the current variations of NO_2 and SO_2 are opposite to those of NH_3, H_2S, and CO since NO_2 and SO_2 usually act as electron acceptors for pentacene. Furthermore, to explore the influence of moisture on the sensing properties, we put the device in the ambient ($RH = \sim 50\%$) for 60 min and then we measure the sensing properties in the same environment. Compared to the results tested in the testing chamber, the variation of I_{on} of these devices is a little lower, exhibiting a 12.5% change to 500 ppb NH_3. Moreover, the device shows deterioration of NH_3 sensing after long time testing in the moisture environment, as shown in Fig. S5, supplementary material, indicating that more efforts are needed to further improve this sensing platform.

In summary, an ultra-sensitive and low-operating voltage organic transistor-based NH_3 sensor was obtained by introducing a gelatin dielectric layer. The change in saturation current achieves 17.6% for the NH_3 concentration of 500 ppb, while the applied operating voltage is only −4 V. Combination of experimental and theoretical results, an excellent LOD of 174.0 ppb for this type of sensor, is demonstrated. Meanwhile, this sensor also presents outstanding selectivity to NH_3. We believe that OTFTs with the biocompatibility and degradation gelatin dielectric layers open an effective way to realize high-performance, low-cost, portable electronic noses.

See supplementary material for capacitance-frequency characteristics, real-time sensitivities, limit of detection, and typical transfer curves, including Figs. S1–S5.

This work was financially supported by the Foundation for Innovation Research Groups of the National Natural Science Foundation of China (NSFC) (Grant No. 61421002), the National Key R&D Program of China (Grant No. 2018YFB0407100-02), the Foundation of NSFC (Grant Nos. 61675041 and 51703019), and City University of Hong Kong (Grant No. 9610423).

[1]R. A. Potyrailo, C. Surman, N. Nagraj, and A. Burns, Chem. Rev. **111**, 7315–7354 (2011).
[2]Y. H. Lee, M. Jang, M. Y. Lee, O. Y. Kweon, and J. H. Oh, Chem **3**, 724–763 (2017).
[3]S. Park, M. Park, S. Kim, S. Yi, M. Kim, J. Son, J. Cha, J. Hong, and K. Yoo, Appl. Phys. Lett. **111**, 213102 (2017).
[4]Z. Wang, L. Huang, X. Zhu, X. Zhou, and L. Chi, Adv. Mater. **29**, 1703192 (2017).
[5]W. Huang, X. Zhuang, F. S. Melkonyan, B. Wang, L. Zeng, G. Wang, S. Han, M. J. Bedzyk, J. Yu, T. J. Marks, and A. Facchetti, Adv. Mater. **29**, 1701706 (2017).
[6]M. Jeon, B. Choi, J. Yoon, D. M. Kim, D. H. Kim, I. Park, and S. J. Choi, Appl. Phys. Lett. **111**, 022102 (2017).
[7]H. Fan, W. Shi, X. Yu, and J. Yu, Synth. Met. **211**, 161–166 (2016).
[8]X. Zhuang, W. Huang, S. Han, Y. Jiang, H. Zheng, and J. Yu, Org. Electron. **49**, 334–339 (2017).
[9]C. Piliego, D. Jarzab, G. Gigli, Z. Chen, A. Facchetti, and M. A. Loi, Adv. Mater. **21**, 1573–1576 (2009).
[10]S. Lai, M. Barbaro, and A. Bonfiglio, Appl. Phys. Lett. **107**, 103301 (2015).
[11]S. Fabiano, H. Yoshida, Z. Chen, A. Facchetti, and M. A. Loi, ACS Appl. Mater. Inter. **5**, 4417–4422 (2013).
[12]S. Han, X. Zhuang, Y. Jiang, X. Yang, L. Li, and J. Yu, Sens. Actuators, B **243**, 1248–1254 (2017).
[13]M. Y. Chuang, C. C. Chen, H. W. Zan, H. F. Meng, and C. J. Lu, ACS Sens. **2**(12), 1788–1795 (2017).
[14]B. Wang, J. Ding, T. Zhu, W. Huang, Z. Cui, J. Chen, L. Huang, and L. Chi, Nanoscale **8**, 3954–3961 (2016).
[15]P. K. Sahu, M. Pandey, C. Kumar, S. S. Pandey, W. Takashima, V. N. Mishra, and R. Prakash, Sens. Actuators, B **246**, 243–251 (2017).
[16]Y. Yang, G. Zhang, H. Luo, J. Yao, Z. Liu, and D. Zhang, ACS Appl. Mater. Inter. **8**, 3635–3643 (2016).
[17]D. Khim, G. Ryu, W. Park, H. Kim, M. Lee, and Y. Noh, Adv. Mater. **28**, 2752–2759 (2016).
[18]W. Huang, K. Besar, R. LeCover, A. M. Rule, P. N. Breysse, and H. E. Katz, J. Am. Chem. Soc. **134**, 14650–14653 (2012).
[19]S. H. Yu, J. Cho, K. M. Sim, J. U. Ha, and D. S. Chung, ACS Appl. Mater. Interfaces **8**, 6570–6576 (2016).
[20]X. Zhou, K. Niu, Z. Wang, L. Huang, and L. Chi, Nanoscale **10**, 8832–8839 (2018).
[21]Z. Wang, Z. Liu, L. Chen, Y. Yang, J. Ma, X. Zhang, Y. Guo, G. Zhang, and D. Zhang, Adv. Electron. Mater. **4**, 1800025 (2018).
[22]W. Huang, J. Yu, X. Yu, and W. Shi, Org. Electron. **14**, 3453–3459 (2013).
[23]S. Ling, C. Li, K. Jin, D. L. Kaplan, and M. J. Buehler, Adv. Mater. **28**, 7783–7790 (2016).
[24]S. Park, Y. J. Kang, and S. Majd, Adv. Mater. **27**, 7583–7619 (2015).
[25]X. Zhuang, W. Huang, X. Yang, S. Han, L. Li, and J. Yu, Nanoscale Res. Lett. **11**, 439 (2016).
[26]J. W. Chang, C. Wang, C. Huang, T. Tsai, T. Guo, and T. Wen, Adv. Mater. **23**, 4077–4081 (2011).
[27]M. İnal, N. Işıklan, and M. Yiğitoğlu, J. Ind. Eng. Chem. **52**, 128–137 (2017).
[28]Y. He, J. Sun, C. Qian, L. Kong, J. Jiang, J. Yang, H. Li, and Y. Gao, Org. Electron. **38**, 357–361 (2016).
[29]Q. Liang, W. Ma, Y. Shi, Z. Li, and X. Yang, Carbon **60**, 421–428 (2013).
[30]W. Wang, J. Xiao, X. Chen, M. Luo, H. Liu, and P. Shao, Food Hydrocolloids **81**, 159–168 (2018).
[31]L.-K. Mao, J. Hwang, T. Chang, C. Hsieh, L. Tsai, Y. Chueh, S. S. H. Hsu, P. Lyu, and T. Liu, Org. Electron. **14**, 1170–1176 (2013).
[32]Y. Seo, J. H. Lee, J. E. Anthony, K. V. Nguyen, Y. H. Kim, H. W. Jang, S. Ko, Y. Cho, and W. H. Lee, Adv. Mater. Interfaces **5**, 1701399 (2018).
[33]C. Zhang, P. Chen, and W. Hu, Chem. Soc. Rev. **44**, 2087–2107 (2015).
[34]X. Yu, L. Zeng, N. Zhou, P. Guo, F. Shi, D. B. Buchhloz, Q. Ma, J. Yu, V. P. Dravid, R. P. H. Chang, M. Bedzyk, T. J. Marks, and A. Facchetti, Adv. Mater. **27**, 2390–2399 (2015).
[35]L. Li, P. Gao, M. Baumgarten, K. Müllen, N. Lu, H. Fuchs, and L. Chi, Adv. Mater. **25**, 3419–3425 (2013).
[36]Q. Wang, S. Wu, F. Ge, G. Zhang, H. Lu, and L. Qiu, Adv. Mater. Interfaces **3**, 1600518 (2016).
[37]W. Shi, J. Yu, and H. E. Katz, Sens. Actuators, B **254**, 940–948 (2018).
[38]M. Y. Lee, H. J. Kim, G. Y. Jung, A. Han, S. K. Kwak, B. J. Kim, and J. H. Oh, Adv. Mater. **27**, 1540–1546 (2015).